

Simulation Study on Self-Focusing Effect of Satellite Laser Communication Under Extreme Ionospheric Conditions

Ning Li

Department of Navigational Technology, Merchant Marine College, Shanghai Maritime University, Shanghai, China

Email address:

15901917996@163.com

To cite this article:

Ning Li. Simulation Study on Self-Focusing Effect of Satellite Laser Communication Under Extreme Ionospheric Conditions. *Journal of Electrical and Electronic Engineering*. Vol. 11, No. 5, 2023, pp. 115-120. doi: 10.11648/j.jeeec.20231105.12

Received: July 19, 2023; **Accepted:** August 23, 2023; **Published:** November 3, 2023

Abstract: Satellite laser communication has developed rapidly, with advantages such as strong anti-interference ability, good confidentiality, high communication rate, freedom from frequency resource constraints, large capacity, small equipment size, low power consumption, and light weight, which can meet the increasingly high requirements for data transmission rate and security in maritime communication. When laser propagates in the ionospheric plasma, the laser pulse undergoes a self-focusing effect. Under extreme conditions such as sudden ionospheric disturbances, the electron density in the ionosphere greatly increases, which has a significant impact on laser transmission. This article analyzes the mechanism of focused beam generation, uses PIC method to simulate the self-focusing effect of laser under extreme conditions in the ionosphere, and studies and determines the method of introducing self-focusing effect in PIC simulation. The self-focusing electric field structure is compared with beams without self-focusing with the same parameters. The results indicate that when laser propagates under extreme conditions in the ionosphere, the front edge of the laser pulse bends, and its laser oscillation frequency increases. In the latter half of the laser pulse, due to the self-focusing effect of the plasma, the width of the laser pulse decreases and the focusing effect is obvious.

Keywords: Satellite Laser Communication, Ionosphere, Self-Focusing, Simulation

1. Introduction

With the development of intelligent shipping and the introduction of the concept of e-Navigation, the requirements for data communication between ships and shore, as well as between ships, are becoming increasingly high. In terms of communication and security, it is necessary to significantly improve the data transmission rate, reliability, and network security of maritime communication. The current maritime mobile satellite communication system has problems such as low communication rate, narrow bandwidth, high cost, and low stability, which will seriously restrict the development of maritime economic activities and scientific research. Satellite laser communication has the advantages of high communication rate, good confidentiality, freedom from the constraints of frequency resources, large capacity, small size, strong anti-interference ability, low power consumption, light weight, etc. [1-4], which can fully meet the needs of modern maritime mobile Internet communication and maritime Information superhighway construction.

The ionosphere is an ionized part of the earth's atmospheric space. Areas in the Atmosphere of Earth with an altitude of more than 60km are in a state of complete or partial ionization, and there are a large number of free electrons and charged ions [5]. The ionospheric region includes the thermosphere and parts of the middle and outer layers, and the region below the ionosphere is called the neutral atmosphere or neutral layer [6, 7]. Since the plasma in the ionosphere is formed by the ionization of atoms and molecules, it is electrically neutral at the macro level [8]. Plasma is the fourth State of matter besides solid, liquid and gaseous substances, and is a common substance in the universe [9]. Plasma exists in the upper atmosphere of the earth, stars and the sun. Plasma has high conductivity and strong coupling with electromagnetic fields. When electromagnetic waves propagate in plasma, scattering, reflection, and refraction effects occur, and changes in the plasma can also have an impact on electromagnetic waves. The ionosphere, as a channel and carrier for electromagnetic wave transmission between satellites and the Earth, is crucial for the quality of laser communication, and research related to

the characteristics of the ionosphere is of great significance.

2. The Self-Focusing Effect of Laser in Plasma

The self-focusing effect occurs when the laser propagates through the plasma [10, 11]. The mechanism of self-focusing is that the laser's mass driving force tends to expel the plasma, and this driving force is opposite to the plasma pressure outside the channel, and the balance between these two causes the plasma density in the channel to decrease, and the decrease in the plasma density increases the refractive index in the channel, thereby focusing the laser beam and preventing its diffusion [12]. Self-focusing results from an increase in the refractive index of a light wave caused by two effects: an increase in electron mass due to the relativistic quiver velocity of electrons in the light wave, and a decrease in electron density due to the mass driven expulsion of electrons. The second effect is also significant in cases where $(P - P_C)/P_C$ is quite small, where P_C is the critical power at which self-focusing occurs and P is the laser beam power. In fact, when $(P - P_C)/P_C \geq 0.1$, the effect is so strong that it ejects all electrons within the core radial region of the self-focusing laser channel (this new phenomenon is known as the electron cavity). [13]

When focused by an optical device with a focal length of f , a beam with an initial diameter of r will be focused at that focal length to a finite waist size ω_0 . The relationship between these three parameters is shown in equation (1) [14].

$$\omega_0 = \frac{2\lambda_L f}{r\pi} \quad (1)$$

In the simulation of laser transmission, some important parameters need to be defined, among which the Rayleigh distance is the distance that the light travels from the beam radius to $\sqrt{2}$ times the beam waist radius [15].

Figure 1 shows the length and related parameters. The confocal parameter b is the distance between $\pm D_R$.

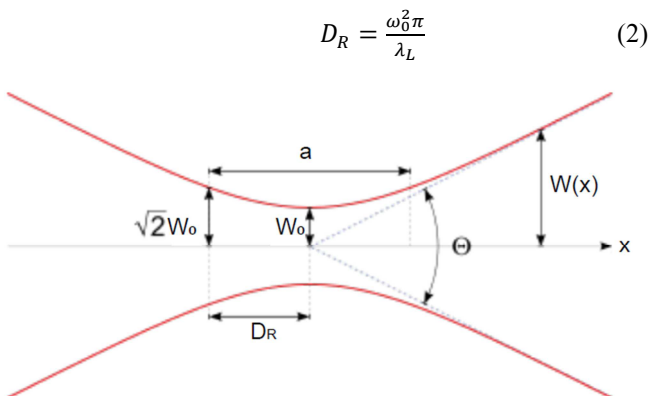


Figure 1. As shown in the figure, the Gaussian contour beam is focused, and the beam is focused to a finite waist size ω_0 . [13].

The focused beam can be obtained by using an equiphase surface curvature radius, which varies as the pulse propagates

with the Guoy phase. The radius of curvature of the focusing Gaussian is as follows [14]:

$$R(x) = \left[1 + \left(\frac{D_R}{x}\right)^2\right] x \quad (3)$$

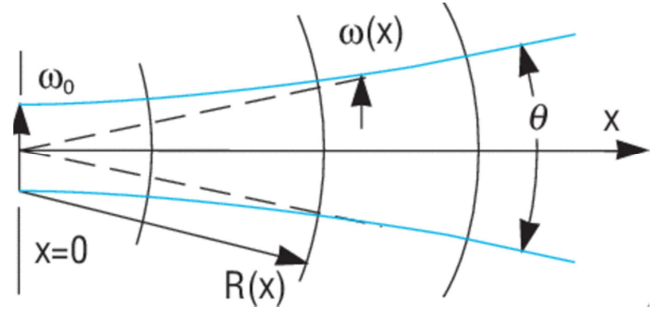


Figure 2. Equiphase surface curvature radius after beam focusing. At the minimum waist radius, the radius of curvature becomes infinite and becomes a straight line.

In Figure 2, several equiphase surface curvature radii are partially superimposed on the waist profile. Another important factor to consider when modeling this system is the change in beam radius (light blue lines in Figure 2). When the electromagnetic wave propagates along the X-axis with R as the radius, the beam radius is shown in equation (4) [14]:

$$\omega_x^2(x) = \left[1 + \left(\frac{x}{D_R}\right)^2\right] \omega_0^2(x) \quad (4)$$

The Guoy phase shift is an additional phase shift produced during the propagation of a focused Gaussian beam. It is increased near the beam waist and is used to focus pulses.

$$\Psi(x) = \arctan\left(\frac{x}{D_R}\right) \quad (5)$$

To achieve focused beam generation, the above relationship is included in the input file of the simulation.

3. Ionospheric Plasma Environment

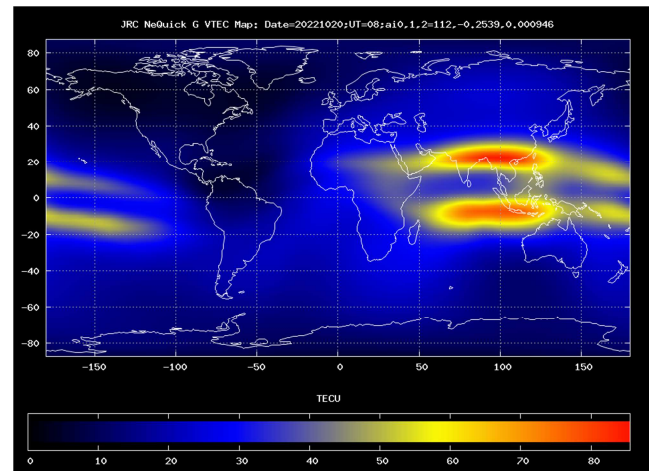


Figure 3. Global ionospheric TEC distribution.

The ionosphere exhibits both regular spatiotemporal changes and significant ionospheric anomalies in both the

time and spatial domains. The main anomalies in the time domain are annual anomalies, semi-annual anomalies, and winter anomalies (or seasonal anomalies). The anomalies in the spatial domain mainly include equatorial anomalies (or Appleton anomalies) and mid latitude valley phenomena [16], as shown in the Figure 3.

The Total Electron Content (TEC) of the ionosphere is closely related to electron density, known as ionospheric electron integral content, concentration column content, etc. It refers to the integration of electron density over height per unit area, represented by TECU, with 1 TECU representing 10^{16} electrons per square meter. TEC is an important parameter for describing the structure and morphology of the ionosphere, and it varies significantly with space and time. The total amount of ionospheric electrons is a very important parameter for ionospheric correction in communication, navigation, and positioning. Changes in TEC will directly affect communication, navigation, and positioning systems. The total amount of electrons in the ionosphere (TEC) plays an important role in the influence of the ionosphere on electromagnetic wave propagation. [16]

The extreme conditions of the ionosphere, such as the sudden disturbance of the ionosphere, also known as the sudden disturbance of the ionosphere, are that when solar flares or coronal mass ejections occur, the solar radiant intensity increases significantly, resulting in a significant increase in the electron density in the lower ionosphere (mainly the D layer), which has a significant impact on radio communication.

4. Simulation Method of Self-Focusing Effect

To investigate the practical impact of self-focusing effect on laser propagation under extreme conditions in the ionosphere, this paper introduces the laser self-focusing effect in the simulation of laser propagation under extreme conditions in the ionosphere using the PIC method,

considering the symmetric Gaussian shaped laser envelope, which is symmetric about the z-axis.

Self-focusing is determined by the phase portion of the laser and the waist profile. Focusing can be thought of as an evolution of spot size and is included in the 'gauss' command. First, the self-focusing phenomenon is simulated, so that the self-focusing electric field structure is compared with the non-self-focusing beam with the same parameters.

In order to capture the evolution process of beam focusing, the simulation parameters need to be modified to improve the resolution on the y-axis and determine the distribution of the changing electric field when the beam converges to the focus point.

The focusing beam parameters are set in the input constant section, and the focusing parameters are calculated using the above relationship and laser parameters.

The laser parameters in the simulation test are as follows:

$$\lambda_L = 1\mu m$$

$$I_L = 8 \times 10^{18} W cm^{-2}$$

$$\tau_L = 26 fs$$

And the focussing parameters by calculation are:

$$\omega_0 = 5\mu m$$

$$f_T = 314\mu m$$

$$D_R = 78.5\mu m$$

$$R_T = 0.334 mm$$

When testing the focusing method, the laser pulses with Gaussian distribution in time and space are focused according to the above conditions. The data is presented in the form of changes in the electric field along the y-axis, and the intensity of the electric field is represented by a smooth contour quantified by a color bar. When the beam enters the simulation area, the curved phase front can be clearly observed, as shown in Figure 4.

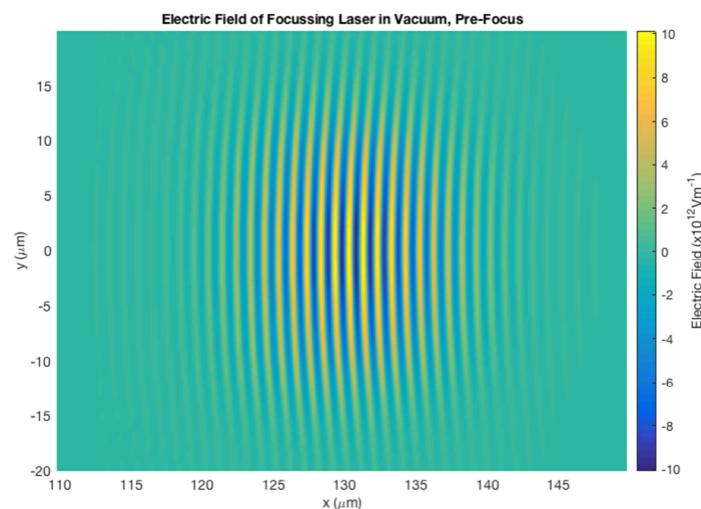


Figure 4. The concave phase front of the adjusted focus can be identified within the pulse envelope. This is the electric field distribution in the y-axis direction before reaching the minimum waist size.

As shown in Figures 5, near the focal point, the laser is contained in a small volume, resulting in the highest laser intensity at the focal point. The curvature radius of the wavefront increases continuously and reaches infinity at the focal point. When the radius of curvature is infinite, the wavefront is flat, then the wavefront begins to flip, and the

phase wavefront bends in the opposite direction. As the pulse moves away from the focus, the radius of curvature decreases, and the pulse diffuses and diffracts in space, as shown in Figure 6, which is consistent with the theoretical diagram of the wavefront form after the focal point shown in Figure 2.

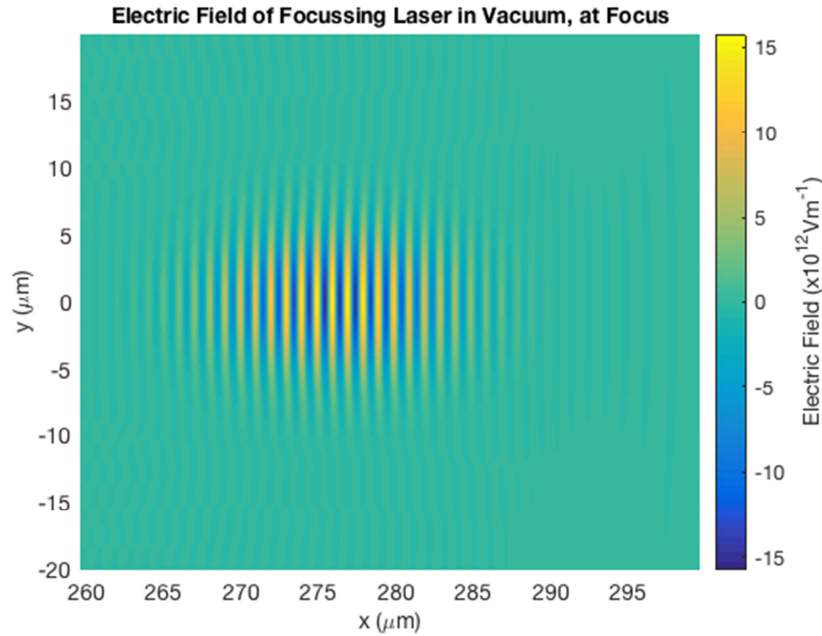


Figure 5. As mentioned above, the focal length is $314\mu\text{m}$, which is slightly before the minimum waist size. The electric field diagram still shows the correlation characteristics.

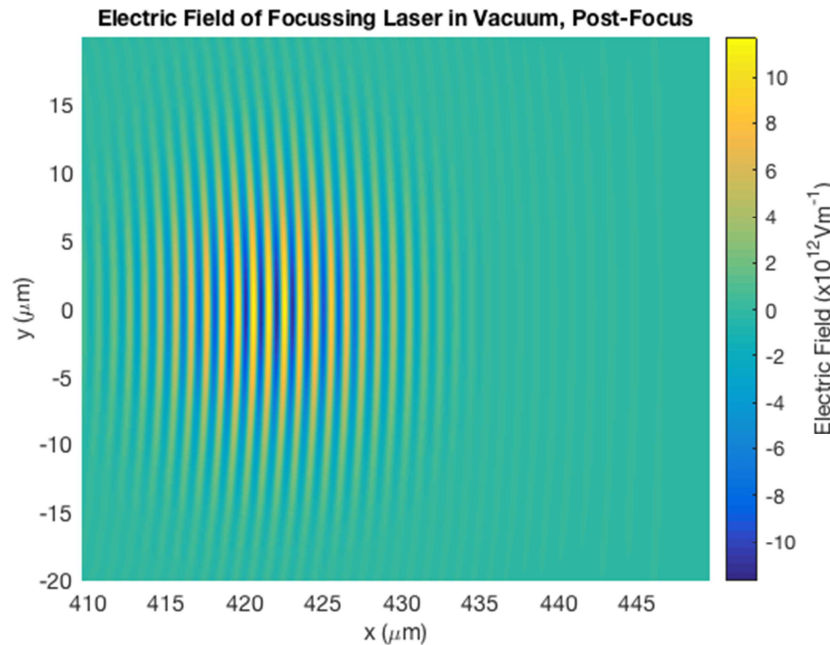


Figure 6. After the focal length is exceeded, the curvature increases again with the pulse diffraction. The energy of the laser occupies an increasing volume, resulting in a decrease in laser intensity.

A collimated beam, such as the one used in previous sections, will not demonstrate any of these features but simply move with a constant spatial profile. The collimated ray in figure 7 shares all the same parameters as the focussing beam

but without the variation in phase and waist profile. The collimated beam then has no curvature to the phase fronts and propagates with a constant spatial envelope.

Collimated beams do not exhibit any of these features, but

simply move in a constant spatial profile. All parameters of the collimated rays in Figure 7 are the same as those of the focused beam, but the phase and waist profile do not change.

The phase wavefront of a collimated beam has no curvature and propagates with a constant spatial envelope.

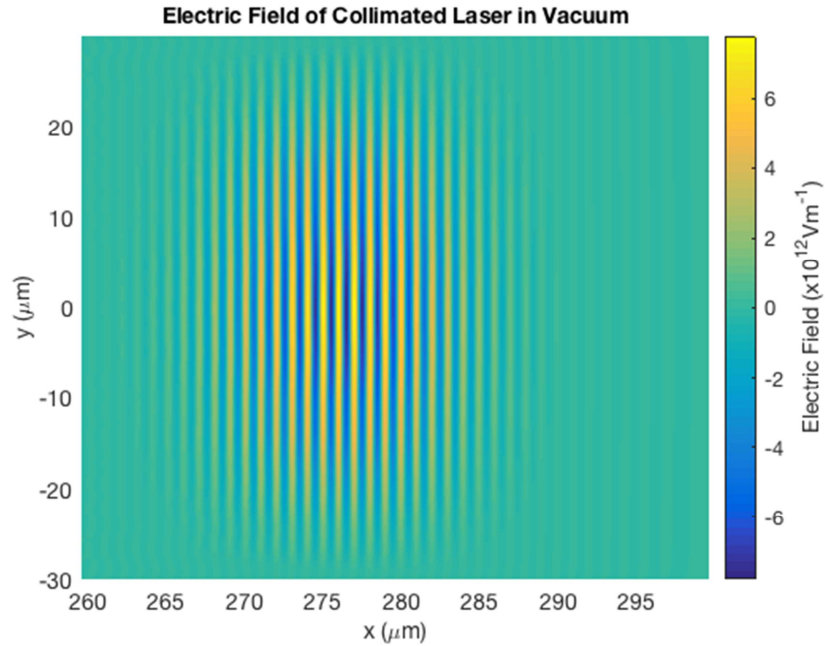


Figure 7. The pulse is a simple collimation line because there isn't the phase space and waist profile change equations. The wavepacket is still limited by diffraction.

5. Simulation of Self-Focusing Effect

The initial intensity of the laser pulse used in this study is $I = \left(6 \times 10^{19} \frac{\text{W}}{\text{cm}^2}\right) \times [(1\mu\text{m}/\lambda_0)^2]$, with a dimensionless amplitude of $a = \frac{eE_0}{\omega m_e c} = 6.62$, propagating forward along the x-axis; Linear polarization along the y-axis direction, with a laser transverse focal spot half height and full width of $10\mu\text{m}$. Pulse width half height full width $35\text{fs} = 10.5T_0$, here ω is the laser frequency, e and m_e is the charge and mass of the electron, E_0 is the size of the laser pulse electric field, c is the speed of light in vacuum, T_0 is the laser period. In this process, the effect of ions can be ignored, i. e. the mass ratio of

ions to electrons is $m_i/m_e \rightarrow \infty$. The simulated window size is $80\lambda_0 \times 80\lambda_0$, the number of grids is 1600×800 , of which $\lambda_0 = 1\mu\text{m}$ is the wavelength of the incident laser in vacuum. Fully ionized plasma distributed at $20\lambda_0 \leq x \leq 100\lambda_0$, with a density of n under extreme ionospheric conditions $n_e = 1.2 \times 10^{18} \text{cm}^{-3} \times \left(\frac{1\mu\text{m}}{\lambda}\right)$. When propagating in a plasma, the waveform evolution of the laser pulse is shown in the following figure 8. Due to the influence of density waves, the front edge of the laser pulse produces a bend resembling a head wave shape, and its laser oscillation frequency increases. In the latter half of the laser pulse, due to the self-focusing effect of the plasma, the width of the laser pulse decreases and the focusing effect is obvious.

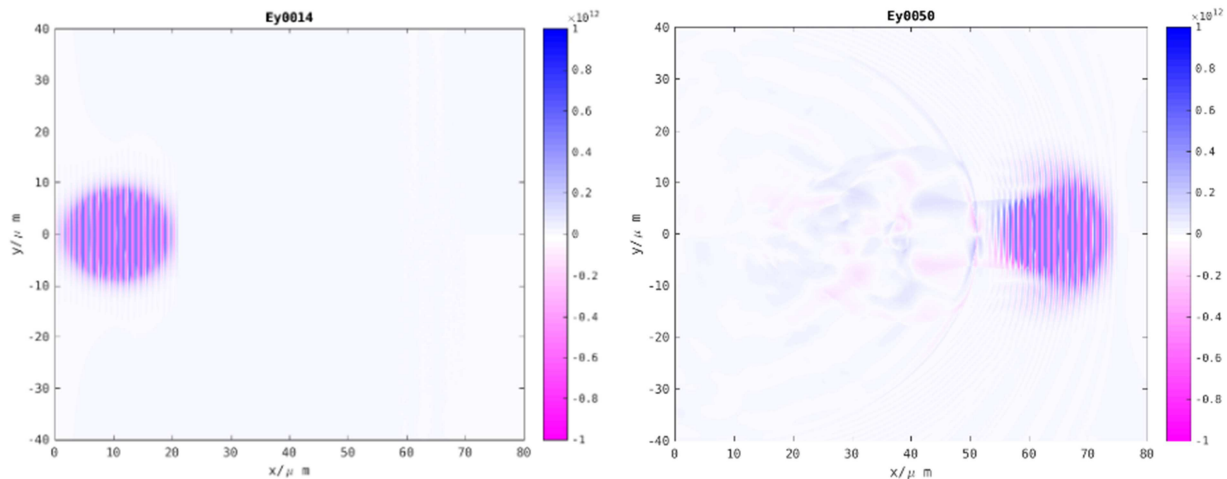


Figure 8. Changes in transverse electric field of laser propagation in space plasma over time, (a) is $14T_0$, (b) is $50T_0$, T_0 is the laser period.

6. Conclusion

This paper uses the PIC method to simulate the self-focusing effect of laser propagation under extreme conditions in the ionosphere. Add self-focusing effect in PIC simulation and compare the self-focusing electric field structure with no self-focusing beams with the same parameters. The results indicate that when laser propagates under extreme conditions in the ionosphere, the front edge of the laser pulse bends, and its laser oscillation frequency increases. In the latter half of the laser pulse, due to the self-focusing effect of the plasma, the width of the laser pulse decreases and the focusing effect is obvious.

References

- [1] M. Toyoshima, W. R. Leeb, H. Kunimori, et al. Comparison of Microwave and Light Wave Communication Systems in Space Application. *Proc. SPIE*. 2005, 5296: 1~12.
- [2] R. G. Marshalek, G. S. Mecherle, P. R. Jordan. System-Level Comparison of Optical and RF Technologies for Space-to-Space and Space-to-Ground Communication Links. *Proc. SPIE*. 1996, 2699: 134~145.
- [3] Guo-An Yan, Hua Lu. Nonreciprocal singlephoton router in quantum networks [J]. *Physica Scripta*. 2021. 96 (10): 105102.
- [4] Wang Chao, Jiang Lun, Keyan Dong, An Yan, Jiang Huilin. Analysis of the Polarization Characteristic of a Satellite-to-Ground Laser Communication Optical System. *Laser & Optoelectronics Progress*. 2015. 52 (12): 120607.
- [5] Yin Weike. Study on the Propagation and Scattering Characteristics of Electromagnetic Waves in Inhomogeneous Plasma [D]. XiDian University. 2020: 13.
- [6] Jones D. Peter Roach, James Hartmann, Jane Setter, eds., *English Pronouncing Dictionary* [M]. Cambridge: Cambridge University Press. 1917.
- [7] Kelly M. The Earth's ionosphere: Plasma physics and electrodynamics [M]. Elsevier, 2012.
- [8] Schunk R W, Walker J C. Theoretical ion densities in the lower ionosphere. *Plant. Sp. Sci.*, 1973, 21 (8): 75-1896.
- [9] Burm, K. T. A. L. Plasma: The Fourth State of Matter. *Plasma Chem Plasma Process* 32, 401–407 (2012).
- [10] Yanfang Li, Jian Wang, N. Yang, Jun-qi Liu, Tao Wang. et al. The output power and beam divergence behaviors of tapered terahertz quantum cascade lasers. *Optics Express*. 2013. 21 (13): 15998-16006.
- [11] Láska, L., Badziak, J., Boody, F., Gammino, S., Jungwirth, K., Krása, J., Wolowski, J. et al. (2007). Factors influencing parameters of laser ion sources. *Laser and Particle Beams*, 25 (2), 199-205.
- [12] Láska, L., Jungwirth, K., Krása, J. et al. Experimental studies of interaction of intense long laser pulse with a laser-created Ta plasma. *Czech J Phys* 56 (Suppl 2), B506–B514 (2006).
- [13] Guo Zheng Sun, etc. Self-focusing of short intense pulses in plasmas [J]. *Phys. Fluids* 30, 526 (1987).
- [14] Masud Mansuripur. *Gaussian Beam Optics*. *Optics and Photonics News*. 2001. 12 (1): 44-45.
- [15] J. Greenwood, 'PHY4025 Part: 1 Ultrafast Atomic & Molecular Dynamics in Intense Laser Fields'.
- [16] Qiang Zhang. Study on the Monitoring of Global Ionospheric TEC Based on Multi-GNSS and Multi-Source Space Observation Techniques [D]. Wuhan University. 2019: 23.